

Design of a Uniform and Tunable Light Source for Photolysis-Based Expansion of 3D Cultured Mesenchymal Stem Cells

A Technical Report submitted to the Department of Biomedical Engineering

Presented to the Faculty of the School of Engineering and Applied Science
University of Virginia • Charlottesville, Virginia

In Partial Fulfillment of the Requirements for the Degree
Bachelor of Science, School of Engineering

Alexandra Julia Rashid

Spring, 2022

Technical Project Team Members

Hannah Bolen

Golnar Mostashari

On my honor as a University Student, I have neither given nor received unauthorized aid on this assignment as defined by the Honor Guidelines for Thesis-Related Assignments

Donald Griffin, Department of Biomedical Engineering

Abstract

Three-dimensional stem cell culture requires scaffolding for cell growth. To harvest the cells for therapeutic or research purposes, the scaffolding must be removed. The current method of degrading the scaffold is enzymolysis, but proteolytic enzymes can degrade the extracellular matrix and surface proteins of stem cells, which is detrimental for stem cell growth, proliferation, and differentiation. A microporous annealed particle (MAP) gel was created that is degradable via application of a 365 nm light which does not harm the cells. However, the current device used to expose the MAP hydrogel scaffold and cells is inefficient, as it can only uniformly expose one well of a 96-well plate at a time. The concept of this project is to create a uniform and tunable light source platform to aid in the photolysis-based expansion of mesenchymal stem cells (MSCs). The light source platform was designed, 3D printed, assembled using LEDs and made uniform using a light diffuser. The final device was tested to show 10.7% variability of light intensity across the area of the 96 well plate. The diffuser provided 4.38 times more uniform light distribution. The longevity of the intensity of the LEDs was tested and had a standard deviation of 0.011 mW/cm². Qualitative gel degradation and quantitative polymer degradation kinetics were conducted to validate the gel degradation capabilities of the device. There was no significant difference in degradation kinetics across the plate, further validating the uniformity. Time trials found a 20-fold time difference between the current device for light exposure and the new light platform. All tests confirmed the light source platform is a uniform source of light that can be used for a more efficient and high throughput degradation of MAP gel scaffolding for the 3D culture of MSCs.

Introduction

Significance of Mesenchymal Stem Cells

Cell-based therapies with mesenchymal stem cells (MSCs) are an exciting avenue of research, especially due to their wide differentiation potential and immunomodulation properties. In the event of a wound or autoimmune disease, MSCs can facilitate repair by secreting growth factors, mobilizing native stem cells, differentiating to assist in structural repair, and through immunomodulation.¹ The bioactive molecules and extracellular vesicles in the MSC secretome are responsible for much of these regenerative and immunomodulatory properties.² The cells are easily derived from the adipose tissue and bone marrow in adults, and therapeutic treatments often rely on autologous transplants which are subjected to minimal FDA oversight.³ This increases the desirability of clinical and translational research of MSCs.

However, there are challenges with the use of MSCs, largely due to the elusive nature of these multipotent stem cells and the inherent heterogeneity in MSC cultures. Questions remain about the native tissue origin and in vivo physiological functions, and there is an incomplete understanding of the underlying mechanisms for the immunomodulatory functions.⁵ Within the field there is no consensus for isolation and expansion protocols, which further contributes to the inherent heterogeneity for these cells.⁶ Distinct cell-to-cell differences in regenerative potential, proliferation potential, and potency are prevalent even within clonal MSC cultures.⁷ Further, there is a demonstrated discrepancy between in vivo and in vitro findings for cellular behavior.⁸ Ultimately, these barriers to research limit the clinical efficacy of in vitro MSC research. These challenges warrant improved characterization of MSCs such that their variable nature can be harnessed for therapeutic purposes, instead of impeding the clinical process. The lack of molecular profiles to consistently identify cell heterogeneity hinders progress in the field and quality control during MSC manufacturing.⁷ In order to better predict the therapeutic potential, improved strategies for large scale MSC cultivation and biobanking must be developed. Effective large-scale cultivation of MSCs is also essential for downstream clinical translation, as an estimated 10^{10} to 10^{13} cells would be needed for a single dose of mesenchymal stem cell-based therapy.⁹

Current Standards of MSC Culturing

There are many considerations that justify the use of 3D culturing methods to study and grow MSCs in vitro. This method of culturing makes it possible for researchers to produce larger quantities of MSCs than is possible with a monolayer culture, and to do so in an environment that better resembles in vivo conditions. This is vital for MSCs since their behavior in vivo must be known before safe clinical

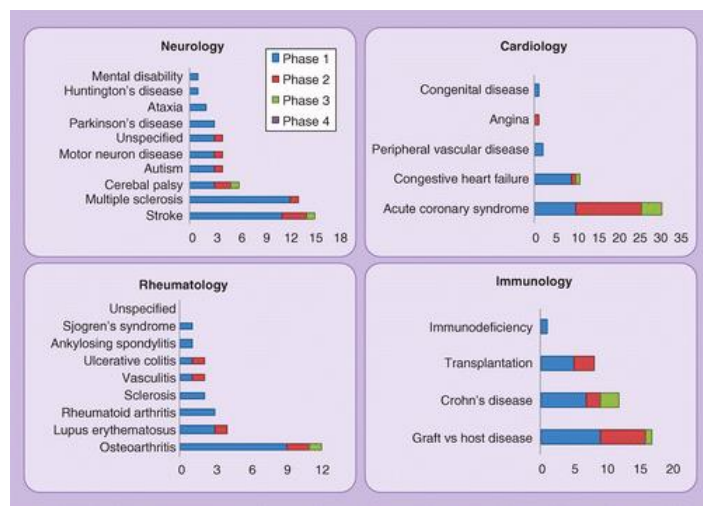


Figure 1. MSC Therapeutic Applications.⁴ Cell therapy clinical trials active in 2015 involving MSCs showing target clinical indications and trial phase.

applications can occur.⁸ It is important to be able to replicate the extracellular matrix, proteins, and signaling since this is thought to be the main mechanism of action for immunomodulatory functions. While this is broadly applicable to many cell culturing techniques, this holds extreme relevance for this project since the platform will be used in conjunction with studies of the secretome's immunomodulatory properties. Therefore, it is essential that the culturing techniques do not alter the secretome and immunophenotype of MSCs.

Current standards for passaging of MSCs in 3D culture require more complex dissociation methods than 2D cultures and rely on proteolytic enzymes. This can decrease the potency, proliferation, differentiation capabilities of the MSCs, which are key features for clinical efficacy. Enzymatic strategies to detach MSCs from the substrate have been demonstrated to alter immunophenotype, which must be avoided to ensure clinical efficacy.¹⁰ While this method allows for high throughput culturing and screening, there are clear drawbacks in the quality of stem cells being harvested.

MAP Hydrogel

The Griffin Lab has created a photosensitive microporous annealed particle (MAP) hydrogel to avoid the aforementioned issues in MSC culturing and scaffold degradation. The photolytic degradation of MAP gel scaffolds with 365 nm wavelength light avoids harming the extracellular proteins and matrices of the MSCs.¹¹ This preserves the stem cell integrity and features that are important for clinical applications, while still effectively degrading the scaffolding. These hydrogel scaffolds must be exposed to a uniform light distribution to ensure consistent scaffold degradation across the area of all wells.

The MAP hydrogel is made of crosslinked polyethylene glycol (PEG) microspheres that form a solid, open pore scaffold.¹² This scaffold contains photodegradable peptide crosslinkers which connect the PEGs to make up microspheres. Additionally, the PEG spheres are adhered together by peptides that attach to these components. When the 365 nm light is administered to the MAP hydrogel, these photodegradable crosslinkers begin to break down. This ensures that the microspheres themselves degrade as well as the connections between the microspheres. While this is promising for use in 3D MSC culturing, the current light device that is used by the Griffin Lab to degrade this scaffolding in a 96-well plate has limitations.

Issues with Degrading MAP Hydrogel

The main issue with the current device is the area of uniform light that it is able to produce. This light source produced a small radius of light that can only uniformly cover the area of one well in a 96-well plate. Additionally, the light is not perfectly sized, so it partially covers the surrounding wells too. This means that only every other well in a 96-well plate can be used if the light is to be uniform across a well, so the scale of experimentation is extremely limited. Each well must be exposed to light for approximately 3 minutes, so 144 minutes is needed to expose all 48 usable wells in the plate to light. This means that to harvest MSCs from 96-wells, approximately 288 minutes, nearly 5 hours, of light exposure is required.

Following light exposure, the plate must be left to incubate while hydrogels degrade. This large duration of light exposure makes the process quite lengthy and inefficient when trying to culture millions of cells at a time. The scalability of the experiments is also limited because plates with larger wells cannot be used since the light source would not uniformly cover the area of the well. This significantly hinders the ability to perform high-throughput experiments, which is imperative for evaluating the effects of a range of factors on the MSCs. Finally, harvesting MSCs with the current device introduces variability as the

experimenter cannot harvest all cells in a plate at the same time. There can be hours between the harvest times of the first and last well, which guarantees that the conditions of the cells in the wells are not identical.

Hypotheses and Aims

The goal of this capstone project was to create and evaluate a functioning uniform and tunable light source platform to allow for higher throughput passaging of MSCs. To accomplish this goal, we had three specific aims. First, to conceptualize the design of the light source platform. Second, to create the physical model of the device by various techniques. And third, to test and validate the effectiveness of the device.

For the first specific aim, conceptualizing the light source platform, the most fundamental aspects of the platform were identified. Physically, the platform had to be scaled to fit under a standard 96-well plate. The light provided by the platform had to shine at a wavelength of 365nm with an intensity range of 0-20 mW/cm² and a uniformity of $\pm < 20\%$ over all wells. For the application of the device, it must be able to be sterilized. The platform was designed using Autodesk Fusion. To ensure the light distribution will be uniform, a light diffuser was acquired to scatter the light intensity throughout the entire area of the well plate. As testing and validation of the device was conducted, changes to the conceptualization and the design of the platform were made to create improved iterations. To approach the design, various pieces were created to have distinct functions to overall form the light source platform.

The second specific aim, to create a physical concept device, was accomplished by 3D printing the various components of the CAD design, purchasing light and electrical components, and soldering the LEDs into a grid. Initially, all pieces of the platform were 3D printed with PLA. After conducting initial tests and validation trials for aim three, adjustments had to be made to the design and materials of the platform. The order of assembly of the final physical device is as follows: a 3D printed PLA base platform to connect all other pieces, a heat sink connected to an aluminum LED plate with a soldered grid of 120 LEDs, followed by an acrylic diffuser case, plastic diffuser, and final 3D printed PLA lid.

For the third specific aim, to validate the effectiveness of the device, the platform was used in four tests. The platform underwent uniformity trials, to ensure that the light intensity is within $\pm < 20\%$ across the well plate. Since the well plate will be on for 15 minutes at a time, extended time trials were conducted to ensure the intensity of light stays constant over the duration of exposure. These tests were performed using a radiometer to track the irradiance over the well and over time. Validity tests were completed to ensure the platform degraded the gel. This test was conducted qualitatively to image the gel degradation after use of the device, and the images were then quantitatively analyzed. Finally, time trials were conducted to ensure the platform allowed for a more efficient way to harvest MSCs.

Results

Platform

The current small device used to degrade the MAP hydrogel is shown in Figure 2A. This light source is mounted on a ring stand and shines light downwards. The plate with gel is placed underneath the light source and must be manually shifted after each individual well is exposed to light. The small circle drawn on the green tape outlines the area that is covered uniformly by the light, which is the area of one well on the 96-well plate.

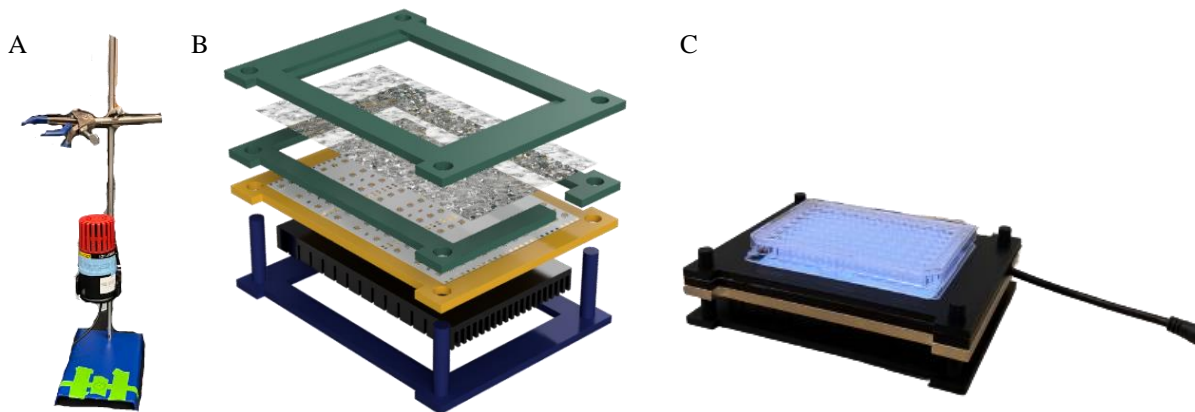


Figure 2. Light Source Platform. A) image of the current light source device used to expose the well plate to light. B) 3D rendering of the new light source platform, from the bottom up, consisting of base platform, a heat sink connected to an aluminum LED plate with a soldered grid of LEDs, diffuser case, diffuser, and diffuser case lid. C) final iteration of the light platform device.

The platform was created using the materials and methods outlined in the previous section. A 3D rendering of the new concept device, and all components are shown in Figure 2B. The final assembly of the platform base, heat sink, aluminum LED plate, acrylic diffuser holder, plastic diffuser, and plastic lid are presented. The LEDs were connected to an external battery, and a dimmer to tune the intensity of the light provided. The final iteration of the device with the LEDs turned on and a representative well plate is shown in Figure 2C. Once assembly was completed, the intensity of light was measured to ensure it fell into the necessary range of 0-20 mW/cm². The probe data seen in Figure 3 for the uniformity trial found that the intensity was on average 3.5 mW/cm² with the diffuser and 14.8 mW/cm² without the diffuser.

Uniformity

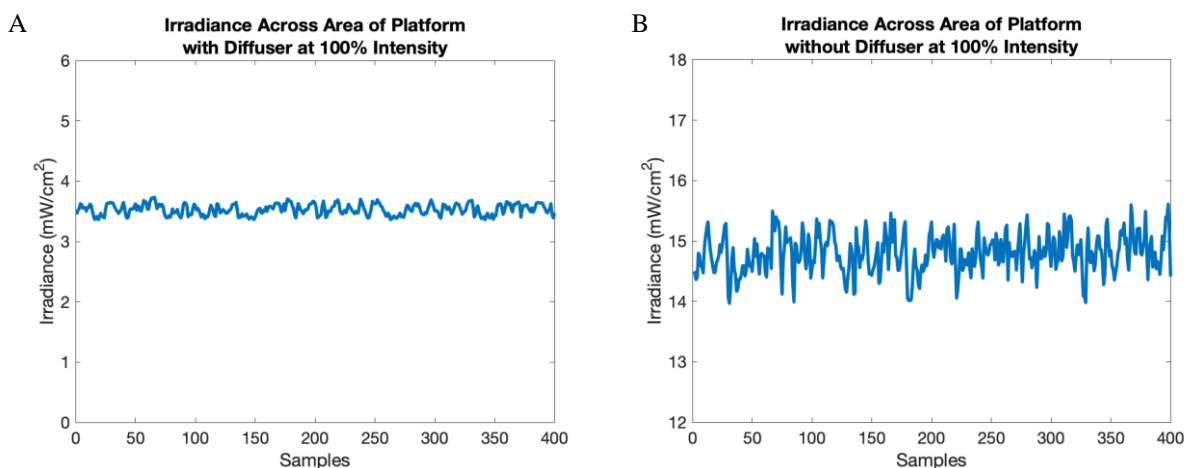


Figure 3. Irradiance Across Area of Platform. A) light intensity was tracked across the area of the well plate with the diffuser. B) light intensity was tracked across the area of the well plate without the diffuser.

In order to evaluate the uniformity of the light produced by the platform, the irradiance (also referred to as light intensity) of the light across the area of the platform was measured. This was conducted using a power meter and probe; the probe was placed where the bottom of the 96-well plate would be and

moved around the area of the platform in a steady and consistent manner. Uniformity trials were performed first with the diffuser at 100% intensity and then without the diffuser at 100% intensity.

$$\text{Equation 1} \quad \textit{variability} = 100 * \frac{\textit{maximum irradiance} - \textit{minimum irradiance}}{\textit{average irradiance}}$$

$$\text{Equation 2} \quad \textit{amplitude} = \textit{maximum irradiance} - \textit{minimum irradiance}$$

$$\text{Equation 3} \quad \textit{residual} = \textit{irradiance}_{\textit{sample } i} - \textit{average irradiance}$$

The standard deviation of the irradiance with the diffuser was 0.1mW/cm² and was 0.3mW/cm² without the diffuser. The variability was then calculated for the platform with and without the diffuser, using Equation 1, and was found to be 10.7% and 11.1%, respectively. Using Equation 2, the irradiance measurements with the diffuser had a calculated amplitude of 0.37 mW/cm², while those without the diffuser had an amplitude of 1.64 mW/cm². The residuals for all data points were found using Equation 3 and then examined for statistical significance. The average of the irradiance residuals without the diffuser was greater than that with the diffuser, with average residuals of 0.257 mW/cm² and 0.0742 mW/cm², respectively. A one-tailed t-test demonstrated that the irradiance residuals for the light source without use of the diffuser are significantly greater than those with the diffuser, with a p-value of $p = 8.47 * 10^{-65}$.

Longevity

Extended time trials were conducted to confirm irradiance produced by the LEDs did not diminish as time progressed. The platform needs to be on for 15 minutes to adequately break the photodegradable bonds of the MAP hydrogel, so it was necessary to validate the longevity of the LED irradiance for this amount of time. The power meter and probe were again used to measure the irradiance. In this experiment the probe was left on the surface of the diffuser and remained in the same spot for the entirety of the 15 minutes.

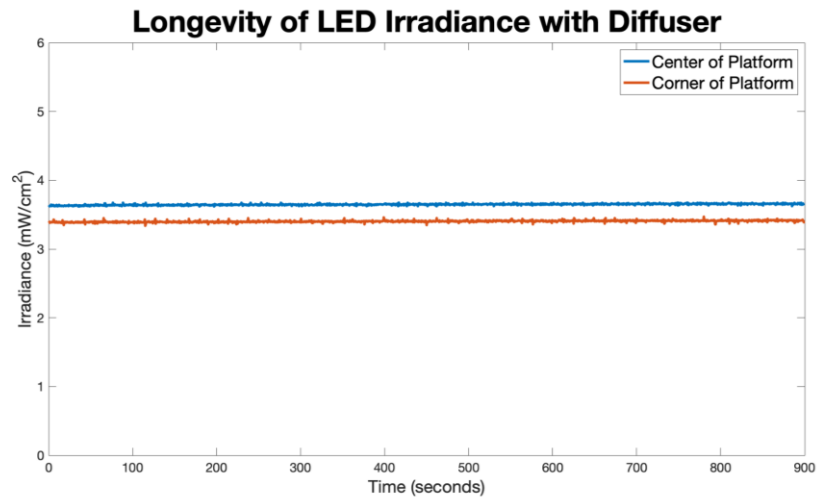


Figure 4. Longevity of LED Irradiance with Diffuser. Extended time trials were conducted for 15 minutes tracking irradiance at the center of the platform and the corner of the platform.

This was done in two places: firstly, in the center of the diffuser and then in the far corner. These locations were chosen to represent two points that would be most distinct from one another. Figure 4 shows the data collected from these trials, with an average irradiance in the center of the platform of 3.6477 mW/cm² and an average irradiance in the corner of the platform of 3.4032 mW/cm². The standard deviation for irradiance in the center of the platform was found to be 0.011237 mW/cm² over the 15 minutes, and the standard deviation in the corner was 0.01333 mW/cm².

Gel Degradation

Once the uniformity and longevity of the LEDs had been investigated and confirmed, experiments were performed to validate the gel degradation ability of the platform. This was performed by plating MAP hydrogel into 32 wells of a 96-well plate. The selected plate layout ensured that there was a well containing the hydrogel in every column and every row to provide a representative model of what the gel degradation of a full plate would look like. The plate layout used is shown in Figure 5A, where each of the wells highlighted in green contained MAP hydrogel.

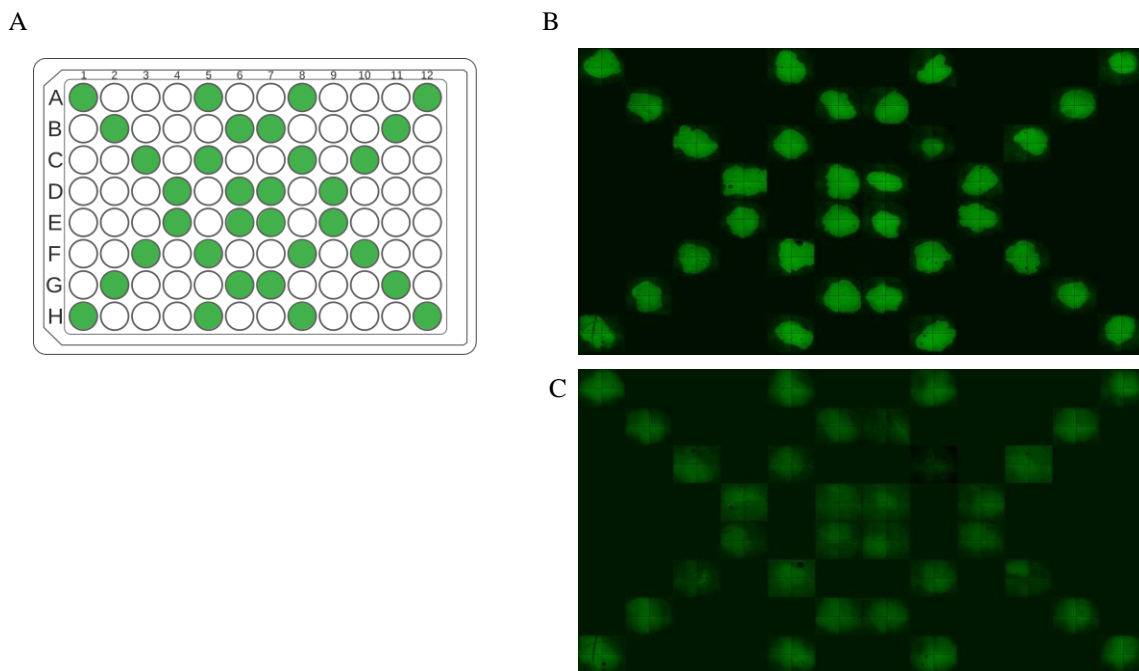


Figure 5. Gel Degradation. A) schematic of the orientation of gel within the 96-well plate for gel degradation trials. B) confocal microscope image of the 96-well plate directly after light exposure. C) confocal microscope image of the 96-well plate after 3 hours after light exposure.

Once the gel was placed in each well and annealed, the 96-well plate was placed on top of the platform and the LEDs were turned on for 15 minutes. During this time, all 96 wells were simultaneously exposed to the light produced by the LEDs. The plate was then placed in a confocal microscope and imaged every 15 minutes for 6.5 hours as the gel fully degraded. This provided representative images of the gel, as seen in Figure 5B, taken immediately after the 15 minutes of light exposure had elapsed, and Figure 5C taken after 3 hours of incubation at room temperature under the microscope on the lab bench. Visually, it can be seen that the distinct shapes of the gels no longer exist in most wells after 3 hours had passed. This is because when the gel degrades into solution, it provides a more uniform green fluorescence in each of the wells that contain MAP hydrogel.

The images taken of each well were also analyzed to quantitatively determine the degradation kinetics. The Griffin lab uses the software MetaXpress from Molecular Devices for the purposes of collecting data that makes it possible to evaluate the degradation of the gels. This software examines the light intensity of every pixel in each image of a specific well. As it analyzes every pixel, it calculates the standard deviation of light intensity for each time point that was imaged. For example, Figure 6 shows the gel degradation of well D6 over the course of 3.25 hours. In the first image, the gel has not begun degrading and therefore there is a large standard deviation of pixel intensities within the image. This is because there are areas of extreme brightness (in the center of the gel) and darkness (areas of the well where no gel was placed or degraded into). In the last image however, the gel has gone entirely into solution and the fluorescence is much more distributed across the image of the well. This makes the light intensity of all of the pixels more similar to one another and therefore the standard deviation between them decreases. This process was repeated for each time point and each well.

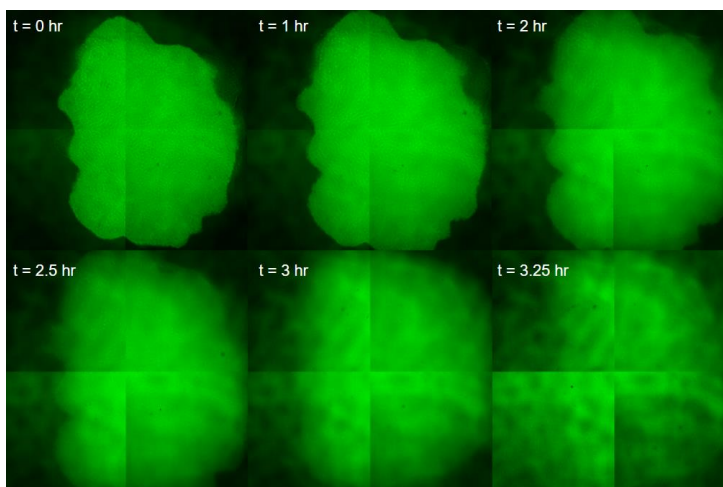


Figure 6. Degradation of Gel in Well D6 Over Time. The degradation of the gel is shown above as the defined outline of the gel becomes more uniform over time throughout the image of the well.

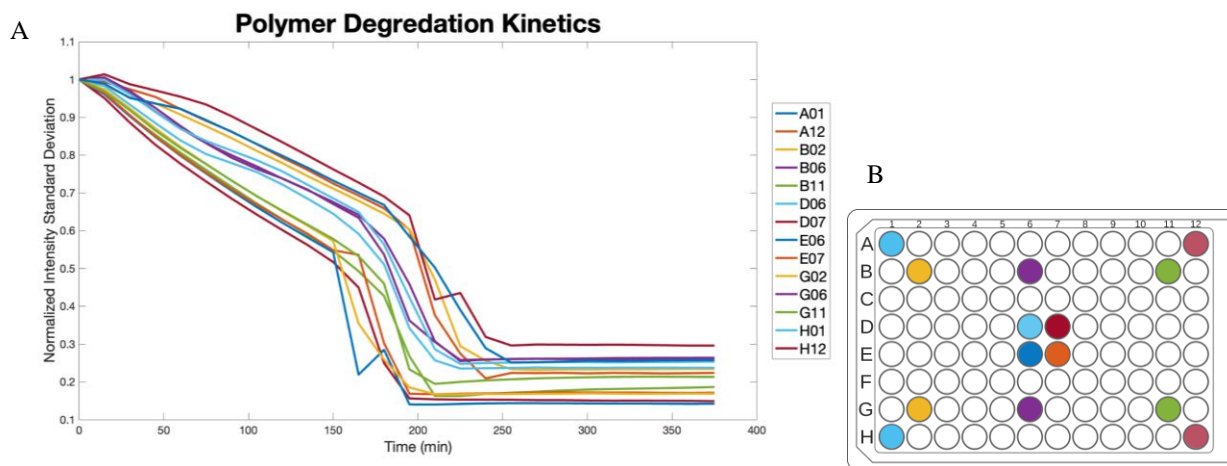


Figure 7. Polymer Degradation Kinetics. A) The normalized intensity standard deviations of 14 wells B) color-coded representative wells used to conduct polymer degradation kinetics.

Once the standard deviations of light intensity for each well were found, they were normalized. This ensured that all standard deviation values for the wells were on the same scale beginning at a value of 1. Doing this allows for a direct comparison of the degradation kinetics for 14 wells of interest (Figure 7). These 14 wells were chosen as they were deemed to be representative of the general kinetics across the 96 well plate. It was important that a representative variety of locations were chosen to analyze kinetics across

the whole area of the 96 well plate. The degradation kinetics of these 14 wells is seen in Figure 7 and displays a steep drop-off in normalized intensity standard deviation near the 200-minute mark. This means that most of the gel had been degraded around 3.5 hours, which is consistent with the visual data seen in the images of the gel degradation. A single factor ANOVA test found no significant difference in degradation kinetics between these 14 wells, with $p = 0.245766359$.

Time Efficiency

One of the main goals of the project, in addition to successfully and uniformly degrading the MAP hydrogel, was to significantly lower the amount of time that was required to expose all wells of a 96 well plate to the LED light. Using the current device, exposing 96 wells containing MAP hydrogel to the uniform light required approximately 288 minutes. With this novel platform, it was determined that only 15 minutes

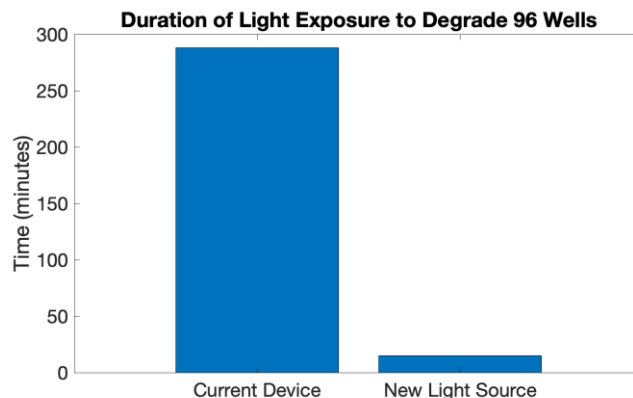


Figure 8. Comparison of Duration of Light Exposure to Degrade 96 Wells. This figure compares the duration of time exposure using the current device, 288 minutes, and the new light source platform, 15

of light exposure was required to initiate the degradation process of the photosensitive peptide crosslinker. As seen in Figure 8, this results in a 20-fold decrease in the time needed to expose 96 wells of hydrogel to this wavelength of light. As mentioned previously, a few hours are still required for the completion of the gel degradation, but the time needed for the complete degradation process has been reduced by over 4 hours with this novel platform.

Discussion

The final iteration of the platform was used to conduct tests to confirm the validity of the device. After conducting initial tests and validation trials, a glaring limitation of the device was identified: the LEDs produce heat, which was not only harmful for the cells, but the heat from the LEDs melted the PLA plastic of the LED plate and the diffuser case. This was remedied by having the LED plate be made of an aluminum sheet, installing a heat sink at the bottom of the LED plate, and creating a diffuser case out of acrylic, which has a higher melting point than PLA.^{13,14} The final iteration of the platform, along with all components and materials, is shown in Figure 2B. The platform build was successful in creating a working, functionalized device. The platform is able to fit all standard sized well plates, for varied applications in the laboratory environment. Additionally, the electronic components are easily separated from the others, making it simple to use 70% ethanol to sterilize the non-electronic parts that come in contact with a well plate.

The uniformity trial was used to confirm the light source had a uniform distribution of light across all wells of the 96-well plate. As seen in Figure 3, the uniformity of irradiance across the platform was significantly increased with the diffuser. This is shown in multiple ways. First, standard deviation of the irradiance with the diffuser was 0.1 mW/cm² and without the diffuser was 0.3 mW/cm². This means that the platform had less variation of intensity with the diffuser, creating a more uniform distribution. Secondly,

the amplitude of the irradiance graph without the diffuser was 1.64 mW/cm^2 , while the amplitude with the diffuser was 0.37 mW/cm^2 . This shows that the platform with the diffuser is 4.38 times more uniform than the platform without the diffuser. These trials further validate the design and confirm that the diffuser is a vital component to ensure uniform light is achieved across the entirety of the well plate when it is placed on the light platform. The variability with and without the diffuser were quite similar, 10.7% and 11.1% respectively. However, the 10.7% variability fits within the requirement for the platform to be uniform $\pm < 20\%$, and therefore proves the design to be successful in the uniformity goal. While the percent variability in light intensity without the diffuser was comparable to the variability with the diffuser, analysis of the residual difference between each irradiance measurement and the mean irradiance showed that the diffuser significantly improved light uniformity. The average residuals were calculated to be 0.0742 mW/cm^2 and 0.257 mW/cm^2 , with the diffuser and without, respectively. The average residual without the diffuser was found to be significantly greater than the average residual with the diffuser. This shows that there is a significant statistical difference between the uniformity of the light source with and without the diffuser and exemplifies the need for the diffuser.

The longevity trials were conducted to ensure the intensity of light does not waiver throughout the 15 minutes that the light source will be shining onto the well plate. As shown in Figure 4, the average irradiance in the center of the platform was 3.6477 mW/cm^2 and the average irradiance in the corner of the platform was 3.4032 mW/cm^2 . The percent difference between these two averages was 6.70%, which is within the goal variability of $\pm < 20\%$. The standard deviation in the center of the platform was 0.011237 mW/cm^2 , and the standard deviation in the corner was 0.01333 mW/cm^2 . These are both exceedingly low values, which illustrates the consistency in the intensity of light being produced in these two areas over the course of 15 minutes.

Gel degradation testing was used to confirm the platform successfully was able to degrade the MAP gel scaffold. These tests verify that the platform is fully functional. To quantify this, polymer degradation kinetics were measured and demonstrated no statistically significant difference in degradation kinetics between the 14 wells analyzed. This further validates the uniformity of the light source platform, as the degradation kinetics for all wells were not significantly different. This means the light was uniformly applied to the MAP gel, to have all the wells degrade at a similar time and rate. Qualitatively and quantitatively, the degradation for all wells occurred after around 3.5 hours. This degradation time is variable and dependent on the amount of crosslinks within the gel itself but is comparable to the time that the gel takes to degrade at room temperature after being exposed using the current device.

While conducting uniformity trials, it was found that the average intensity of the light source platform with the diffuser was 3.5 mW/cm^2 . While this is within the goal range of up to 20 mW/cm^2 , the current device has an intensity of approximately 20 mW/cm^2 . Since this platform has an intensity that is approximately five times lower than the current device, the time of exposure needed to be increased by a factor of five. The exposure time of the current device was three minutes per well, so the new platform had to be in use for 15 minutes for the total plate. The total duration of light exposure for *all* 96-wells for the current device was summed to be 288 minutes. This is nearly 5 hours, which is not able to support effective and efficient high throughput MSC passaging and can result in variability in the cells across the wells. Therefore, the 15 minutes for the new light source platform made a 20-fold difference in exposure time for *all* 96-wells (Figure 8). This definitively improves the efficiency of the degradation process.

Conclusions

The platform created was found to be a functional, tunable, and uniform light source to aid in the degradation of MSCs. The uniformity was validated via quantitative irradiance measurements, and with the diffuser the platform was found to have $\pm 10.7\%$ uniformity. The addition of the diffuser was found to create a statistically significant difference in the uniformity of the light. The longevity was validated via quantitative irradiance measurements, which found that over the course of the 15 minutes the platform would be in use the deviation in irradiance was minute. The gel degradation capabilities were qualitatively and quantitatively found to be sufficient, and the degradation kinetics were shown to be uniform across the platform. Finally, the time needed to expose 96 wells of MAP hydrogel to the light was significantly decreased 20-fold to improve the efficiency of harvesting MSCs. These results show the platform was successful in creating a uniform and tunable light source platform to allow for higher throughput passing of MSCs.

Materials & Methods

Physical Model

The physical components of this platform were created using 3D printing, water jetting, and laser cutting. The base and diffuser case top were designed in Autodesk Fusion 360 and then 3D printed out of PLA plastic using Ultimakers at the University of Virginia. The LED platform and diffuser case bottom were also designed in Autodesk Fusion 360, but these components were created differently. The LED platform was cut out of aluminum using a water jet in Lacy Hall. The diffuser case bottom was laser cut out of acrylic in Stacey Hall since it rested directly on top of the LED platform and was directly exposed to heat from the LEDs. The light shaping diffuser was ordered from Luminit to ensure a uniform distribution of light. Additionally, an aluminum heat sink was purchased and glued to the back of the LED platform to help further draw heat away from the LEDs.

Electronics

The electronic components used were strips of 365 nm LEDs, a dimmer, and a power supply, all purchased from Waveform Lighting. These were connected to provide the tunability of the light source platform that was desired. The led strips were cut and adhered to the LED platform to cover the area of the 96-well plate. These were then soldered together in series.

Light Source Testing

The main method of validating the platform's uniformity and longevity involved taking irradiance data using a ThorLabs power meter and probe. For the uniformity trials, the probe was placed above the platform where the bottom of the 96-well plate would sit. The platform was then turned on and the probe was manually moved around the opening where the light shined while taking readings every half second for three minutes, for a total of 400 samples. To investigate the longevity, the same probe was used but it was left stationary in one location for 15 minutes rather than moving it around the area.

Degradation Trials

Finally, assessing the gel degradation capabilities of the platform was done using a confocal microscope and the software MetaXpress from Molecular Devices at the Griffin lab that analyze the intensity of each pixel in an image. This software examines the light intensity of every pixel in each image of a specific well.

As it analyzes every pixel, it calculates the standard deviation of light intensity for each time point that was imaged. Areas of extreme brightness (in the center of the gel) and darkness (areas of the well where no gel was placed or degraded into) will have a large standard deviation. After degradation has occurred and the fluorescence is distributed across the image of the well, the light intensity of all the pixels is more similar to one another and therefore the standard deviation between them decreases. This process was repeated for every image of each well at each time point. This allowed for a comparison of the pixel intensity across each image, and the standard deviation between these values to be calculated. The standard deviations were normalized by dividing each of the 27 time points for a given well by the first time point and then plotted against time, to assess when the full degradation of the gel occurred. This allowed for a direct comparison of the degradation kinetics for 14 wells of interest.

References

1. Balaji, S., Keswani, S. G. & Crombleholme, T. M. The Role of Mesenchymal Stem Cells in the Regenerative Wound Healing Phenotype. *Adv. Wound Care* **1**, 159–165 (2012).
2. Wangler, S. *et al.* Uncovering the secretome of mesenchymal stromal cells exposed to healthy, traumatic, and degenerative intervertebral discs: a proteomic analysis. *Stem Cell Res. Ther.* **12**, 11 (2021).
3. Regulatory Considerations for Human Cells, Tissues, and Cellular and Tissue-Based Products: Minimal Manipulation and Homologous Use; Guidance for Industry and Food and Drug Administration Staff., 28.
4. Heathman, T. R. *et al.* The translation of cell-based therapies: clinical landscape and manufacturing challenges. *Regen. Med.* **10**, 49–64 (2015).
5. Gomez-Salazar, M. *et al.* Five Decades Later, Are Mesenchymal Stem Cells Still Relevant? *Front. Bioeng. Biotechnol.* **8**, (2020).
6. Gao, F. *et al.* Mesenchymal stem cells and immunomodulation: current status and future prospects. *Cell Death Dis.* **7**, e2062 (2016).
7. O'Connor, K. C. Molecular Profiles of Cell-to-Cell Variation in the Regenerative Potential of Mesenchymal Stromal Cells. *Stem Cells Int.* **2019**, e5924878 (2019).
8. Song, N., Scholtemeijer, M. & Shah, K. Mesenchymal Stem Cell Immunomodulation: Mechanisms and Therapeutic Potential. *Trends Pharmacol. Sci.* **41**, 653–664 (2020).
9. Marklein, R. A., Mantay, M., Gomillion, C. & Warnock, J. N. Biomanufacturing of Mesenchymal Stromal Cells for Therapeutic Applications. in *Cell Culture Engineering and Technology: In appreciation to Professor Mohamed Al-Rubeai* (ed. Pörtner, R.) 267–306 (Springer International Publishing, 2021). doi:10.1007/978-3-030-79871-0_9.
10. Cherian, D. S., Bhuvan, T., Meagher, L. & Heng, T. S. P. Biological Considerations in Scaling Up Therapeutic Cell Manufacturing. *Front. Pharmacol.* **11**, (2020).
11. Wong, D. Y., Ranganath, T. & Kasko, A. M. Low-Dose, Long-Wave UV Light Does Not Affect Gene Expression of Human Mesenchymal Stem Cells. *PLoS ONE* **10**, e0139307 (2015).

12. Griffin, D. R., Weaver, W. M., Scumpia, P., Di Carlo, D. & Segura, T. Accelerated wound healing by injectable microporous gel scaffolds assembled from annealed building blocks. *Nat. Mater.* **14**, 737–744 (2015).
13. Vouyiouka, S. N. & Papaspyrides, C. D. 4.34 - Mechanistic Aspects of Solid-State Polycondensation. in *Polymer Science: A Comprehensive Reference* (eds. Matyjaszewski, K. & Möller, M.) 857–874 (Elsevier, 2012). doi:10.1016/B978-0-444-53349-4.00126-6.
14. Staff, C. M. Everything You Need To Know About Acrylic (PMMA). <https://www.creativemechanisms.com/blog/injection-mold-3d-print-cnc-acrylic-plastic-pmma>.